Laser assisted positronium formation in positron collision with Rydberg hydrogen

M. K. Matfunjwa, H. B. Ambalampitiya, and I. I. Fabrikant
Department of Physics and Astronomy, University of Nebraska, Lincoln, Nebraska 68588-0299, USA
(Dated: November 22, 2024)

We investigate the formation of positronium (Ps) in the presence of a linearly polarized infrared laser field, via the collision of positrons with Rydberg hydrogen atoms H(n_H) where n_H is the principal quantum number. We are using classical trajectory Monte Carlo method (CTMC) which is justified for $n_H \geq 3$. In the presence of the external laser field, the hydrogen in excited states has an effective dipole moment which leads to a dipolar focusing [H.B. Ambalampitiya, M.K. Matfunjwa and I. I. Fabrikant, *J. Phys. B: At. Mol. Opt. Phys.* **57**, 10LT01 (2024)]. Due to this effect, the Ps formation cross section is enhanced substantially as compared to the zero-field case. The degree of this enhancement is controlled by the positron velocity, laser frequency and the laser-field amplitude. The final-state distribution in Ps is much broader than in the zero-field case.

I. INTRODUCTION

Positron (e^+) is a stable antimatter counterpart of the electron. It is stable in a vacuum, however it annihilates when interacting with matter. The positron can bind to an electron to form positronium [1]. Positronium is a purely leptonic atom with a lifetime that depends on its quantum state: 125 ps for the ground state singlet (para-Ps), $^1S_0$ and 142 ns for the triplet state (ortho-Ps), $^3S_1$. On the atomic time scale the lifetimes of the positron and Ps are long enough to lead to interactions of practical importance.

Processes involving Ps, in particular reactions

$$e^+ + \mathrm{H}(n_\mathrm{H} l_\mathrm{H}) \to \mathrm{Ps}(n_\mathrm{Ps} l_\mathrm{Ps}) + p \tag{1}$$

$$e^- + \bar{\mathrm{H}}(n_{\bar{\mathrm{H}}} l_{\bar{\mathrm{H}}}) \to \mathrm{Ps}(n_\mathrm{Ps} l_\mathrm{Ps}) + \bar{p}. \tag{2}$$

are important for antihydrogen studies [2–8]. Reactions of the first type are used in Ps scattering experiments [9–11] whereby Ps beam is formed by the electron transfer from a neutral target to positron. Production of Ps in excited states is important for many other experiments, particularly for precision optical and microwave spectroscopy of Ps [12, 13], as well as Ps-Ps interaction in confining medium [14–16].

External electric fields have been shown to influence atomic processes. This has led to a wide range of applications in atomic physics. In the laser-assisted collisions of electrons with ions, the Coulumb focusing effect has been predicted. In particular, the Coulumb focusing has been shown to strongly affect processes of bremsstrahlung, radiative recombination, and dissociative recombination [17–19]. In collisions of positrons with excited hydrogen atoms, the inclusion of the laser field leads to the dipolar focusing effect [20]. The basic idea and some illustrative examples of the dipolar focusing occurring in positron collisions with H atom in the $n_H = 3$ state were presented in [20].

In the present paper we investigate this effect more systematically. We present extensive calculations for the case when the hydrogen atom is in the states with the principal quantum numbers 4 and 5. We also analyze a realistic case of the wavelengths corresponding to the CO_2 laser and moderate intensities typical for storage-ring experiments [21–23]. We also study the final-state distribution which turns out to be much broader than in the zero-field case, similar to what happens in the process of the hydrogen formation in Ps-p collisions [24].

We use atomic units unless stated otherwise.

II. THEORY

A. CTMC method

Classical treatment of e^+ collisions with the H(n_H) atom was shown [20] to be valid for $n^2 \gg 1$. Specific calculations for various n_H and their comparison with fully quantum-mechanical calculations [25] performed by the convergent close coupling method showed that the classical results agree with quantum ones starting from $n_H = 3$. Hence we employ the classical trajectory Monte Carlo (CTMC) method which has been used to describe three-body collisions since the pioneering work of Abrines and Percival [26]. It has been applied to study hydrogen (antihydrogen) formation without an external field [27–29] and the laser-assisted process as well [24].

In our treatment of the problem, we consider a linearly polarized laser field and we use the dipole approximation to describe the interaction of the positron and the electron with the laser field. The field's time dependence is given by

$$\mathbf{F}(t) = \mathbf{e} F_0 \cos(\omega t + \phi_0), \tag{3}$$

where F_0 is the field amplitude, ω is the angular frequency and ϕ_0 is the phase of the field at the instant when the positron enters the field region ($t = 0$). The Ps formation cross section should be averaged over ϕ_0 which is equivalent to the average over all instances of electron entrance in the field region [18]. The vector $\mathbf{e}$ is the laser polarization vector and the initial velocity $\mathbf{v}_0$ of the positron beam is taken to be along this vector, as the dipolar focusing is most efficient for the parallel geometry similar to what have been found for the Coulomb focusing [30]. Far away from the target the positron performs

the quiver motion with the mean velocity

$$\bar{v} = v_0 - \frac{F_0}{\omega}\sin\phi_0, \tag{4}$$

where v_0 is the positron velocity at $t = 0$. The positron will only approach the target if $\bar{v}$ is positive. From Eq. (4), we obtain the condition $0 < \phi_0 < \phi_1$ or $\pi - \phi_1 < \phi_0 < 2\pi$, where

$$\phi_1 = \arcsin\chi, \quad \chi = \frac{\omega v_0}{F_0}. \tag{5}$$

However, this estimate does not incorporate e^+ - H attraction. Calculations show that even for slightly negative $\bar{v}$ collisions are possible due to the dipolar attraction. The basic conclusion is that the dipolar focusing, like Coulomb focusing [18, 30] is efficient if the parameter χ is less or equal to 1, or slightly exceeds 1.

The Ps formation cross section is calculated by integrating the probability of the process over the impact parameter b and averaging over the phase as

$$\sigma = \frac{1}{2\pi}\int \sigma(\phi_0)d\phi_0, \tag{6}$$

$$\sigma(\phi_0) = 2\pi\int P(b)bdb, \tag{7}$$

where $P(b) = N_{\rm Ps}(b)/N(b)$ is the probability of Ps formation given by the ratio of the number of trajectories leading to the Ps formation to the total number of trajectories for a given impact parameter. We propagate the solutions of the Hamiltonian of the system for enough time. Then we collect statistics by checking the final angular momenta and energies for different channels. From these statistics we calculate the probabilities and subsequently the cross section.

B. Phase average

In Fig. 1, we present the Ps formation in e^+ - H($n_{\rm H} = 4$) collision as a function of the phase ϕ_0. As ϕ_0 approaches ϕ_1 or $\pi - \phi_1$, the cross section diverges strongly. Even the average over ϕ_0 results in an infinite cross section, similar to the case of the Coulomb focusing [18]. In real experimental conditions it might become finite due to instrumental functions as discussed in Refs. [18, 20] For example, if the duration of the laser pulse t is finite, for large enough impact parameters the positron would not reach the target during the time period t, and this would provide the cross section cut-off. This cut-off mechanism is employed in the present paper.

A finite pulse duration affects cross section for phases close to ϕ_1 and $\pi - \phi_1$, therefore in our calculations we introduce a finite pulse duration when ϕ_0 satisfies two conditions, $0 < \phi_1 - \phi_0 < 0.2$ or $0 < \phi_0 - (\pi - \phi_1) < 0.2$. For example if $\chi = 0.832$, $\phi_1 = 0.982$, and for $\phi_0 = 0.98$, when the pulse duration is $t = 200$ ps, the Ps formation cross section is 9.3×10^5 a.u. It reduces to 8.1×10^4 a.u. and 5.5×10^4 a.u. for $t = 10$ ps and $t = 5$ ps, respectively. We stress that we choose the finite pulse duration in ps region to simplify computations, but the longer is the pulse the stronger is the dipolar focusing effects and the larger is the cross section.

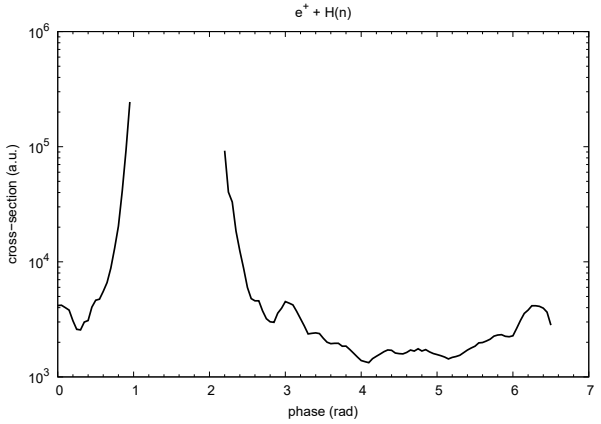

FIG. 1. Cross section for Ps formation in e^+ - H($n_{\rm H} = 4$) collision as a function of phase ϕ_0 for $E = 0.14$ eV, $F_0 = 2.44 \times 10^{-4}$ a.u. and $\omega = 0.002$ a.u. Note the divergencies at $\phi_0 = \phi_1$ and $\phi_0 = \pi - \phi_1$.

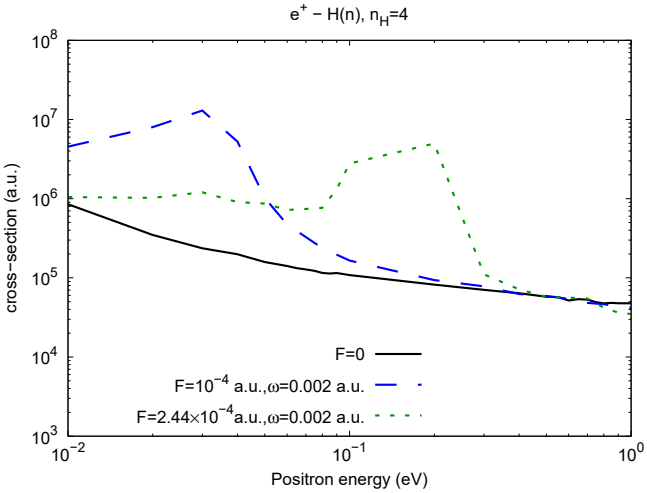

FIG. 2. Ps formation cross section in e^+ - H($n_{\rm H}$) collision as a function of positron energy E for $n_{\rm H} = 4$. Parameters ω and F_0 in a.u. are given in the legend.

III. RESULTS AND DISCUSSION

A. Total cross sections

In this section we present our results for Ps formation for the field amplitude F_0 in the range between 0.2×10^{-4} a.u. and 2.0×10^{-4} a.u. These correspond to intensities between 14.0 MW/cm^2 and 1.4 GW/cm^2. In Fig. 2, we present the phase-averaged Ps formation cross section for $n_{\rm H}=4$, as a function of energy in the range of the positron energy between 0 and 1 eV. We show results for the field-free case and the non-zero field cases, $F_0=10^{-4}$ a.u. and $F_0=2.44\times10^{-4}$ a.u. The laser-assisted Ps formation cross section exhibits a peak at $E=0.04$ eV and $E=0.2$ eV respectively. These energies correspond to $\chi=1$. Above this energy the critical phase does not exist and the dipolar focusing effect gradually becomes less important.

The Ps formation cross section exhibits a strong enhancement compared to the zero-field case. In particular for positron energy $E=0.2$ eV and field amplitude $F_0=2.44\times10^{-4}$ a.u. the cross section is 0.475×10^7 a.u., which is a factor of 58.0 higher than in the zero-field case. At higher energies the gain factor is decreasing, and the presence of the field can lead even to a suppression of the formation of positronium in the region around $E=1$ eV.

To investigate the enhancement further, we look at the Ps formation probabilities. In Fig. 3, we present the Ps formation probability as a function of the impact parameter b for the e^+ - H($n_{\rm H}=4$) collision for the positron energy $E=0.14$ eV. We observe that the probability for Ps formation in the zero field is greater than for the nonzero field for low impact parameters, but it decreases quickly and does not extend to higher impact parameters like in the nonzero-field case. Fluctuation of the probability are attributed to statistical uncertainties of the CTMC calculations. A large number of trajectories is used to minimize the statistical errors. However, chaotic behavior and fractal structures in the $P(b)$ dependence, observed in the laser-assisted Coulomb scatteing [18], are not present here.

In Fig. 4, we present the xz projection of the trajectories for a positron and an electron for e^+ - H($n_{\rm H}$) collisions. The impact parameter vector is directed along the x axis, and the initial velocity $\mathbf{v}_0$ along the z axis. In the present example we take $F_0=10^{-4}$ a.u., $\omega=0.002$ a.u. and the impact parameter is $b=300$ a.u. The positron velocity is $v_0=0.0484$ a.u. corresponding to energy 0.032 eV, so that $\omega v_0/F_0=0.970$. The phase is $\phi_0=1.28$, which is close to the critical phase $\phi_1=1.325$ for this field intensity. For the field-free case the positron trajectory is not affected by the presence of the hydrogen atom. In the non-zero field case the positron performs a quiver motion and eventually gets dragged toward the target excited atom even for large impact parameters. Note that at the initial part of the trajectory the positron is repelled by the target which corresponds to orientation of the atomic dipole towards the positron, but eventually

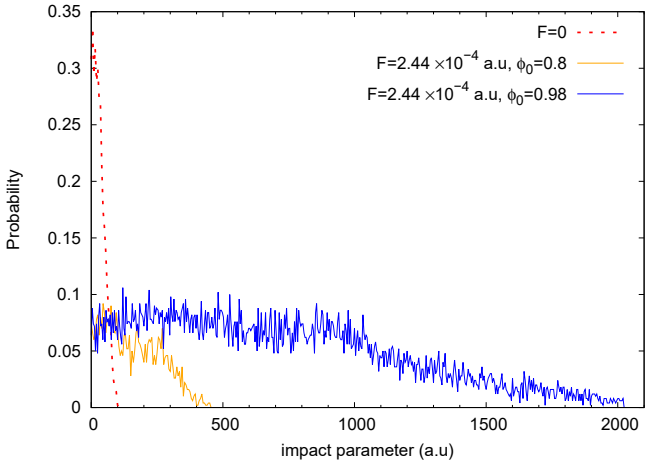

FIG. 3. Ps formation probability in e^+ - H(n) collisions for $E=0.14$ eV. The red dotted line: e^+, $F_0=0$. The orange and blue lines: $\phi_0=0.8$ and $\phi_0=0.98$ respectively, for $F_0=2.44\times10^{-4}$ a.u, $\omega=0.002$ a.u.

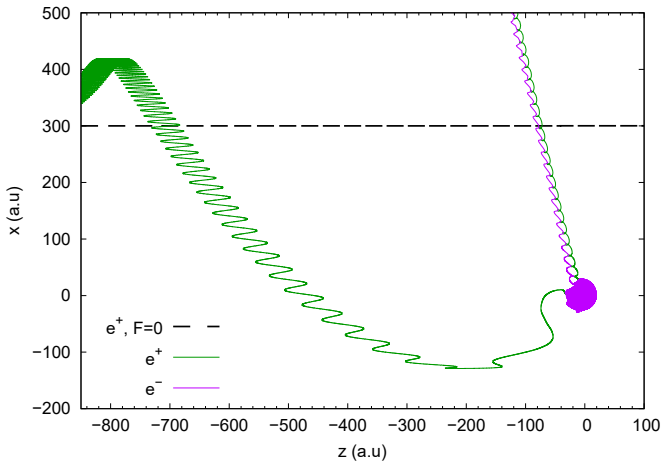

FIG. 4. xz projection of positron and electron trajectories in e^+ - H($n_{\rm H}=4$) collisions for $b=300$ a.u. Green and purple lines: e^- and e^+ trajectories for $F_0=10^{-4}$ a.u, $\omega=0.002$ a.u., $\phi_0=1.29$. The electron orbit parameters are chosen at random; the positron trajectory is shown by the green line, and electron trajectory by the purple line. The field is along the z axis, and the impact parameter vector is along the x axis.

positron gets attracted due to change of the orientation of the dipole.

For $n>4$ the field with the amplitude $F_0=2.44\times10^{-4}$ a.u. ionizes the target hydrogen atom while the positron is still far from the target. Therefore for $n_{\rm H}=5$ we choose lower field amplitude, $F_0=2.44\times10^{-5}$ a.u. and the frequency in the far infrared region, $\omega=0.0002$ a.u., so that $\omega v_0/F_0=0.832$. We present sample trajectories

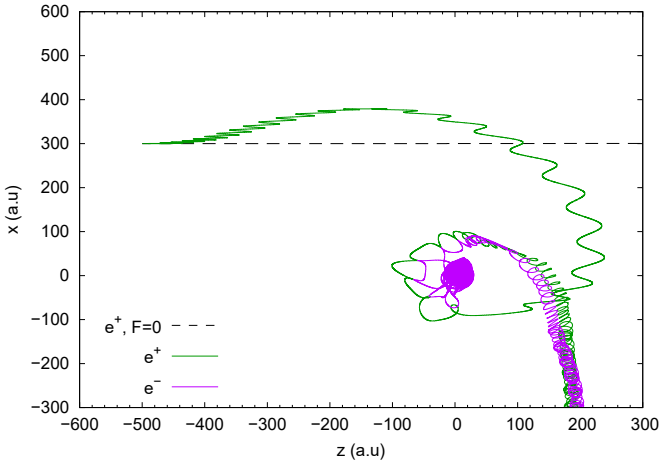

FIG. 5. xz projection of positron and electron trajectories in $e^+ - \mathrm{H}(n_\mathrm{H}=5)$ collisions for $b = 300$ a.u., and $E = 0.02$ eV. Black line: e^+, $F_0 = 0$; purple and green lines: e^- and e^+ trajectories for $F_0 = 2.44\times10^{-5}$ a.u, $\omega = 0.0002$ a.u., $\phi_0 = 0.8$ and a random choice of the parameters of the electron orbit.

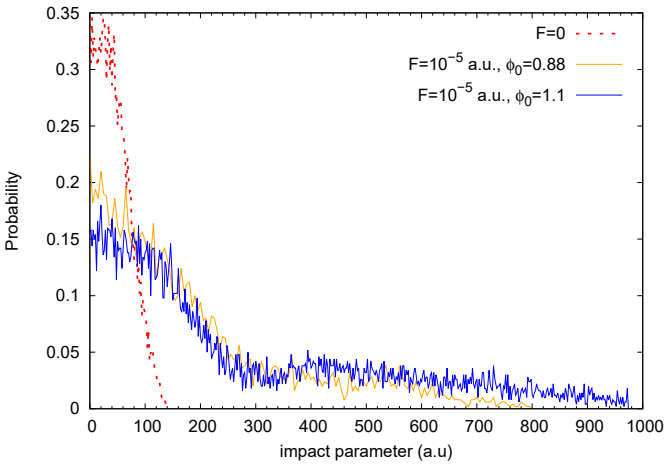

FIG. 6. Ps formation probability in $e^+ - \mathrm{H}(n_\mathrm{H})$ collisions for $n_\mathrm{H} = 5$. Black line: e^+, $F_0 = 0$ with positron energy $E = 0.03$ eV. The orange and blue lines: $\phi_0 = 0.88$ and $\phi_0 = 1.10$ respectively, for $F_0 = 10^{-5}$ a.u, $\omega = 0.0002$ a.u.

for this case in Fig. 5. As in the $n_\mathrm{H} = 4$ case, we take the impact parameter to be $b = 300$ a.u., and we observe again that the field promotes Ps formation, in contrast to the field-free case. We also present the probability of Ps formation for $n_\mathrm{H} = 5$ in Fig 6. Here we show again the field-free and nonzero-field probabilities for the charge transfer for collision of the e^+ and $\mathrm{H}(n_\mathrm{H})$ at positron energy $E = 0.02$ eV. In this case we show probability for the field amplitude $F_0 = 10^{-4}$ a.u., frequency $\omega = 0.0002$ a.u., and phases $\phi_0 = 0.88$ and $\phi_0 = 1.10$.

In Figs. 7 we show the Ps formation cross section as a function of energy for $n_\mathrm{H} = 5$. With our choice of laser parameters, the dipolar focusing effect is operative in the energy range from 10^{-2} to 1 eV. The cross section for the non-zero field case is typically higher than in the zero-field case in this region. The cross sections for $F_0 = 2.44 \times 10^{-5}$ a.u. and $F_0 = 10^{-5}$ a.u. exhibit peaks at positron energies $E = 0.2$ eV and $E = 0.03$ eV respectively. The cross section at these energies is 6.89×10^5 and 1.67×10^7 respectively, which is a factor of 2.8 and 31.9 higher than the field free case. For low energies, the presence of the field can lead to a suppression in the cross section for the field amplitude $F_0 = 2.44 \times 10^{-5}$ a.u., while for $F_0 = 10^{-5}$ a.u., the enhancement on the cross section gradually becomes stronger.

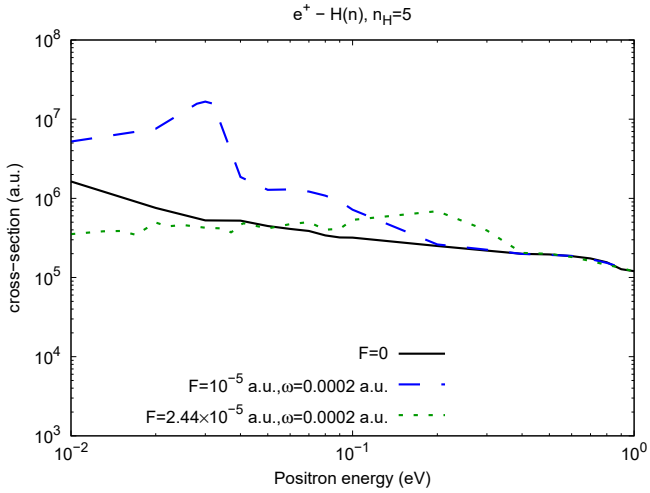

FIG. 7. Ps formation cross section in e^+ - $\mathrm{H}(n_\mathrm{H})$ collisions as a function of the positron energy E for $n_\mathrm{H} = 5$. ω and F_0 indicated in the legend in a.u.

B. Final-state distribution in n_Ps

For a fixed initial hydrogen quantum number, n_H, the charge transfer process produces a distribution of the Ps final-state principal quantum numbers n_Ps. In Fig. 8 we present the Ps formation cross section as a function of n_Ps for $n_\mathrm{H} = 4$. The peak in the zero-field Ps formation cross section satisfies the resonance condition,

$$n_\mathrm{Ps} = \frac{n_\mathrm{H}}{\sqrt{2}}.$$

The resonance condition corresponds to the electron binding energies in the initial and final states being approximately equal. This was also observed in hydrogen/antihydrogen formation in Ps-p/Ps-$\bar{p}$ collisions [24, 27] and is typical for heavy-particle collisions [32]. In the non-zero field case the distribution is broadened.

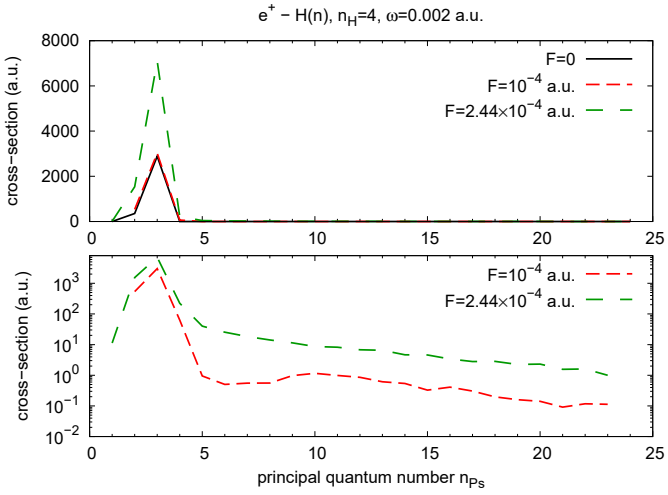

FIG. 8. Cross section for Ps formation in e^+ - H($n_{\rm H}$), $n_{\rm H} = 4$ collision as a function of principal quantum number, $n_{\rm Ps}$ for various field amplitudes, positron energy $E = 0.14$ eV, and $\omega = 0.002$ a.u. Upper panel: linear plot. Lower panel: semilog plot.

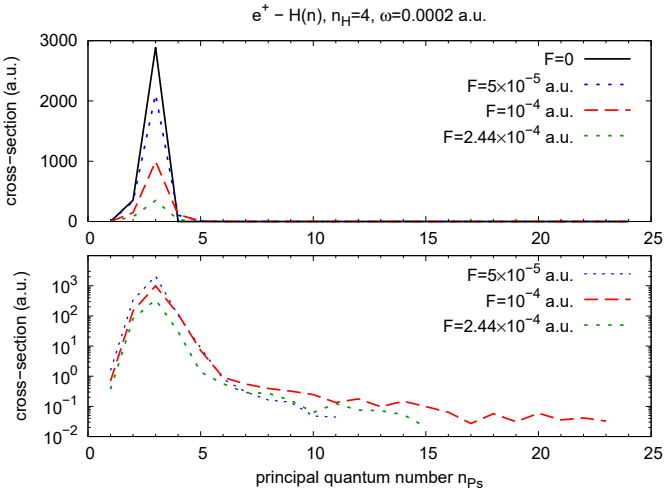

FIG. 9. Cross section for Ps formation in e^+ - H($n_{\rm H}$), $n_{\rm H} = 4$ collision as a function of principal quantum number, $n_{\rm Ps}$ for various field amplitudes, positron energy $E = 0.14$ eV, and $\omega = 0.0002$ a.u. Upper panel: linear plot. Lower panel: semilog plot.

The cross section is nonzero even for higher $n_{\rm Ps}$, the region where the field-free cross section is zero due to the conservation of energy. However, the cross section is relatively small at higher $n_{\rm Ps}$. To demonstrate the $n_{\rm Ps}$ distribution in this region, we also plot it on a log scale. We are interested in a broadening of the distribution and a possible shift of the peak of the distribution to higher $n_{\rm Ps}$ which was observed in Ps-p collisions [24]. The distribution becomes broader with the increasing intensity. The cross section is also enhanced when compared to the zero field case for some intensities. We do not, however, observe a clear shift in the peak of the distribution.

In Fig. 9, we show the final-state distribution in $n_{\rm Ps}$ for far infrared frequency $\omega = 0.0002$ a.u. The lower frequency leads to further broadening of the distribution and the peak reduction. Adjusting the field intensity and the frequency accordingly can be used to obtain a broader distribution. More specifically, the distribution for $F_0 = 2.44 \times 10^{-4}$ a.u. exhibits a peak that is higher than that for the zero-field distribution for $\omega = 0.002$ a.u. For $\omega = 0.0002$ a.u. the peak is lower than in the zero-field case. These effects result from the positron's (or electron's) energy exchange with the field. Similar effects are observed for $n_{\rm H} = 5$. This is illustrated in Figs. 10 and 11, where we show the final-state distribution for two frequencies $\omega = 0.002$ a.u. and $\omega = 0.0002$ a.u.

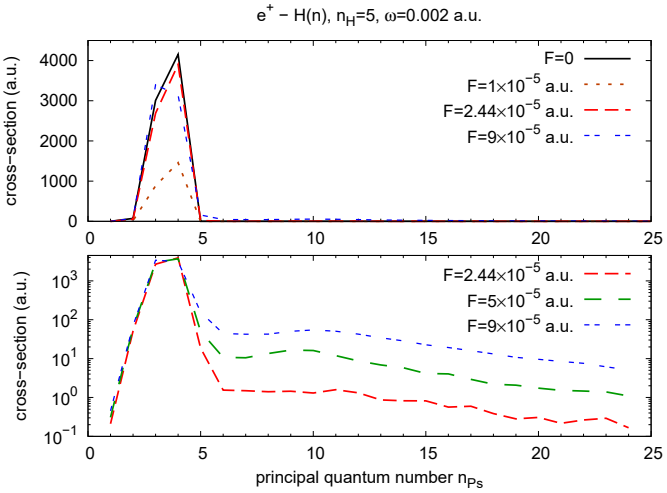

FIG. 10. Cross section for Ps formation in e^+ - H($n_{\rm H}$), $n_{\rm H} = 5$ collision as a function of principal quantum number, $n_{\rm Ps}$. For varying field amplitute, positron energy $E = 0.14$ eV, and $\omega = 0.002$ a.u. Upper panel: linear plot. Lower panel: semilog plot.

C. Final-state distrinbution in $l_{\rm Ps}$

We also perform an analysis of the final state distribution in the orbital angular momentum quantum number, $l_{\rm Ps}$. In Fig. 12, we show the cross section for Ps formation as a function of $l_{\rm Ps}$ that is, show a set of $l_{\rm Ps}$ distributions for different $n_{\rm Ps}$ values. We observe that the distributions exhibit peaks for $l_{\rm Ps}$ closer to the corresponding $n_{\rm Ps}$, meaning that circular orbits are more likely to be formed similar to the case of laser-assisted charge transfer in Ps-$p/\bar{p}$ collisions [24]. This might be beneficial for Ps collision experiments since the circular orbits are more stable radiatively.

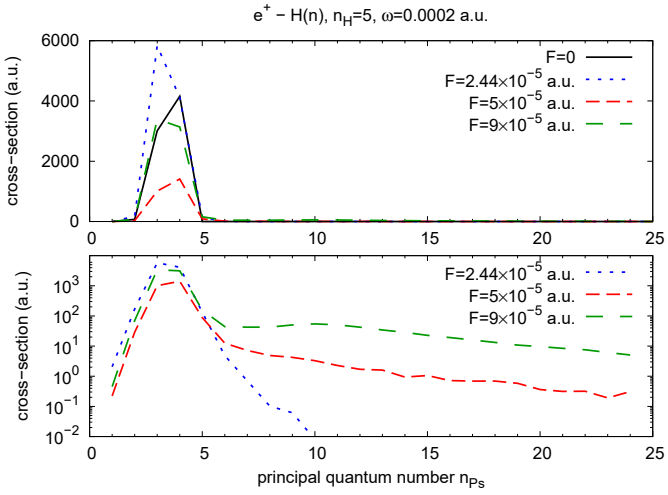

FIG. 11. Cross section for Ps formation in $e^+ + \mathrm{H}(n_\mathrm{H})$, $n_\mathrm{H} = 5$ collision as a function of principal quantum number, n_Ps. For varying field amplitute, positron energy $E = 0.14$ eV, and $\omega = 0.0002$ a.u. Upper panel: linear plot. Lower panel: semilog plot.

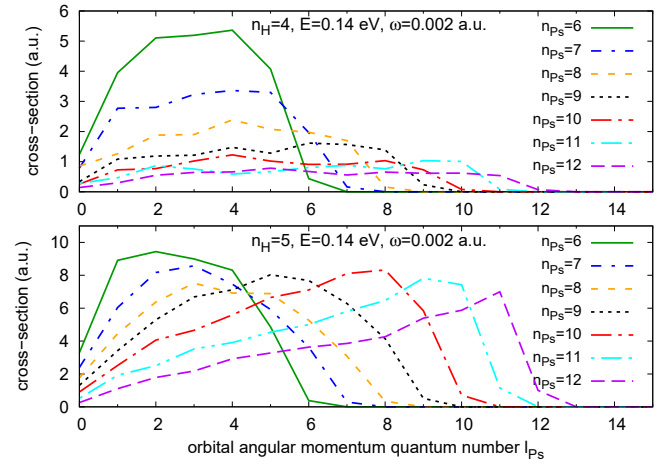

FIG. 12. Cross section for Ps formation in e^+ - $\mathrm{H}(n_\mathrm{H})$ collision as a function of orbital angular momentum quantum number, l_Ps, for $n_\mathrm{H} = 4$ and 5 for various field amplitudes, positron energy $E = 0.14$ eV, and $\omega = 0.002$ a.u.

D. The CO_2 laser parameters

The CO_2 laser, commonly used in laser-assisted collisions [33], emits a mid-infrared wavelength that ranges between 9.3 μm and 10.6 μm corresponding to frequencies ω ranging from 0.00478 a.u to 0.00431 a.u.. In this section we present calculations for these laser parameters in the positron energy region where the dipolar focusing effect is important. The CO_2 laser has been used for laser assisted electron-atom collision, more specifically low energy electron collision with helium atoms [34], where three intensities were used, 38.0 MW/cm^2, 13.0 MW/cm^2 and, 4.2 MW/cm^2 corresponding to the field amplitudes 0.33×10^{-4}, 0.19×10^{-4} and, 0.11×10^{-4} a.u. respectively. Short pulses can increase the radiation intensity output of the TEA CO_2 laser even further [35].

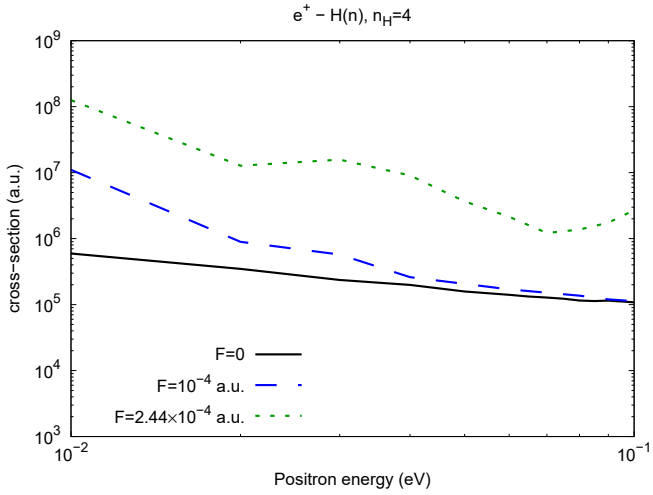

FIG. 13. Ps formation Cross section for in e^+ - $\mathrm{H}(n_\mathrm{H})$ collision as a function of positron energy E. For the CO_2 laser where $n_\mathrm{H} = 4$, $\omega = 0.0043$ a.u. and F_0 indicated in the legend.

In Fig. 13, we show the phase averaged cross section for Ps formation for the zero field and the nonzero-field cases. In the latter case the field amplitudes are $F_0 = 2.44 \times 10^{-4}$ a.u. and $F_0 = 10^{-4}$ a.u., and the frequency $\omega = 0.00431$ a.u., following the example of [33]. The positron energy varies between 10^{-2} and 10^{-1} eV. For positron energy $E = 0.03$ eV, there is an enhancement in the laser assisted Ps formation cross sections of the order of 2.4 and 66.6 for the $F_0 = 10^{-4}$ a.u. and $F_0 = 2.44 \times 10^{-4}$ a.u., respectively. The cross section peaks at energies corresponding to $\chi = 1$. For low energies, the enhancement become stronger.

In Fig. 14, we show the Ps formation cross section for the CO_2 laser as a function of the Ps principal quantum number n_Ps for positron energy $E = 0.03$ eV. In our illustration of the final state distribution we took the positron energy to be 0.03 eV corresponding a positron velocity of 0.0470 a.u., so that $v_0\omega/F_0 = 0.828$.

IV. CONCLUSION

Due to the dipolar interaction between the positron and the excited hydrogen atom, low-energy e^+–$\mathrm{H}(n_\mathrm{H})$ collisions can be treated classically provided that $n^2 \gg 1$[20]. This allowed us to employ the CTMC method to calculate the laser-assisted Ps formation cross section in e^+ - $\mathrm{H}(n_\mathrm{H})$ collisions. The presence of the laser field leads to an enhancement factor ranging 3 to 67, even

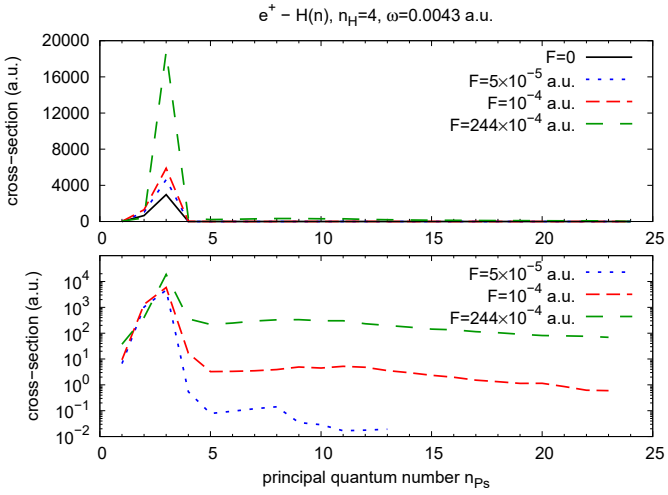

FIG. 14. Cross section for Ps formation in e^+ - H($n_{\rm H}$) collision as a function of principal quantum number, $n_{\rm Ps}$, for the CO_2 laser parameters. Upper panel: linear plot. Lower panel: semilog plot.

for intensity as low as 20.9 MW/cm^2, in the low-energy region between 0.01 and 1 eV.

An important observation is the absence of chaos in this problem, which was observed in the laser-assisted radiative recombination problem [18] and other processes involving the Coulomb interaction [17, 19]. Our final-state distribution analysis shows that formation of circular orbits with $l_{\rm Ps}$ close to $n_{\rm Ps}$ is more favorable.

The present treatment can be extended to the processes of Ps formation in positron collisions with excited atoms other than hydrogen. These processes are of practical importance for the purpose of Ps formation in anti-hydrogen studies [7] and for the formation of Ps beams in studies of Ps collisions with atoms and molecules [9–11].

[1] M. Deutsch, *Phys. Rev.* **82**, 455 (1951).
[2] C. H. Storry, A. Speck, D. Le Sage, N. Guise, G. Gabrielse, D. Grzonka, W. Oelert, G. Schepers, T. Sefzick, H. Pittner, M. Herrmann, J. Walz, T. W. Hänsch, D. Comeau, and E. A. Hessels, *Phys. Rev. Lett.* **93**, 263401 (2004).
[3] M. Charlton and D. P. van der Werf, *Science Progress*, **98**, 34 (2015).
[4] W. A. Bertsche, E. Butler, M. Charlton, and N. Madsen, *J. Phys. B: At. Mol. Opt. Phys.* **48**, 232001 (2015).
[5] C. Amsler *et al.*, *Comm. Phys.* **4**, 19 (2021).
[6] P. Adrich *et al.*, *Eur. Phys. J. C*, **83**, 1004 (2023).
[7] G. Gabrielse, *Adv. At. Mol. Opt. Phys.* **50**, 155 (2005).
[8] H. B. Ambalampitiya, D. V. Fursa, A. S. Kadyrov, I. Bray, and I. I. Fabrikant, *J. Phys. B: At. Mol. Opt. Phys.* **53**, 155201 (2020).
[9] G. Laricchia, S.A. Davies, M. Charlton, T.C. Griffith, *J. Phys. E: Sci. Instrum.* **21**, 886 (1988).
[10] A.J. Garner, A. Özen, G. Laricchia, *Nucl. Instrum. Methods Phys. Res. Sect. B* **143**, 155 (1998).
[11] S.J. Brawley, S.E. Fayer, M. Shipman, G. Laricchia, *Phys. Rev. Lett.* **115**, 223201 (2015).
[12] D. B. Cassidy, *Eur. Phys. J. D* **72**, 53 (2018).
[13] T. J. Babij, D. B. Cassidy, *Eur. Phys. J. D* **76**, 121 (2022).
[14] D. B. Cassidy and A. P. Mills, Jr. *Phys. Rev. Lett.* **107**, 213401 (2011).
[15] D. B. Cassidy and A. P. Mills, Jr. *Phys. Rev. Lett.* **100**, 013401 (2008).
[16] D. B. Cassidy, S. H. M. Deng, R. G. Greaves, T. Maruo, N. Nishiyama, J. B. Snyder, H. K. M. Tanaka, and A. P. Mills, Jr. *Phys. Rev. Lett.* **95**, 195006 (2005).
[17] H. B. Ambalampitiya and I. I. Fabrikant, *Phys. Rev. A* **99**, 063404 (2019).
[18] I. I. Fabrikant and H. B. Ambalampitiya, *Phys. Rev. A* **101**, 053401 (2020).
[19] I. I. Fabrikant, H. B. Ambalampitiya, and I. F. Schneider, *Phys. Rev. A* **103**, 053115 (2021).
[20] H. B. Ambalampitiya, M. K. Matfunjwa and I. Fabrikant, *J. Phys. B: At. Mol. Opt. Phys.* **57** 10LT01 (2024).
[21] U. Schramm, J. Berger, M. Grieser, D. Habs, E. Jaeschke, G. Kilgus, D. Schwalm, A. Wolf, R. Neumann, R. Schuch, *Phys. Rev. Lett.* **67**, 22 (1991).
[22] A. Wolf, *Hyp. Interact.* **76**, 189 (1993).
[23] A. Scrinzi, N. Elander, A. Wolf, *Z. Phys. D* **34**, 185 (1995).
[24] H. B. Ambalampitiya, J. Stallbaumer, and I. I. Fabrikant *Phys. Rev. A* **105**, 043111 (2022)
[25] H. B. Ambalampitiya, J. Stallbaumer, I. I. Fabrikant, I. Kalinkin, D. V. Fursa, A. S. Kadyrov, I. Bray, *Phys. Rev. A* **108**, 032808 (2023)
[26] R. Abrines and I. C. Percival, *Proc. Phys. Soc.* **88**, 873 (1966).
[27] D. Krasnicky, G. Testera, and N. Zurlo, *J. Phys. B: At. Mol. Opt. Phys.* **52**, 115202 (2019).
[28] M. Charlton, H. B. Ambalampitiya, I. I. Fabrikant, D. V. Fursa, A. S. Kadyrov, I. Bray, *Phys. Rev. A* **104**, L060803 (2021).
[29] M. Charlton, H. B. Ambalampitiya, I. I. Fabrikant, I. Kalinkin, D. V. Fursa, A. S. Kadyrov, I. Bray, *Phys. Rev. A* **107**, 012814 (2023).
[30] I. I. Fabrikant and H. B. Ambalampitiya, *J. Phys. B: At. Mol. Opt. Phys.* **57**, 195201 (2024).
[31] D. Krasnický, R. Caravita, C. Canali, and G. Testera, *Phys. Rev. A* **94**, 022714 (2016).
[32] J. B. Delos, *Rev. Mod. Phys.* **53**, 287 (1981).
[33] N. J. Mason, *Rep. Prog. Phys.* **56** 1275 (1993).
[34] B. Wallbank and J. K. Holmes, *J. Phys. B: At. Mol. Opt. Phys.* **27** 1221 (1994).
[35] Y. N. Panchenko, V. F. Losev, A. V. Puchikin, and Y.

Jun, *Russian Physics Journal* **56**, 1246 (2014).